Protein Cell 2017, 8(10):762–766
DOI 10.1007/s13238-017-0463-x

Protein & Cell

LETTER

Structural and biochemical characterization of DAXX-ATRX interaction

Dear Editor,

Epigenetic factors, acting as co-activators/repressors in transcription, regulate diverse cellular activities ranging from cell growth and differentiation to host defense and immune response. Covalent histone or DNA modifications, histone variants, ATP-dependent chromatin remodeling, and non-coding RNA are major mechanisms underlying epigenetic regulation. In particular, ATP-dependent chromatin remodeling complexes and histone chaperones are key factors that regulate chromatin dynamics.

Death domain-associated protein (DAXX), originally identified as a Fas death receptor binding protein during apoptosis, was characterized as an H3.3-specific histone chaperone to promote replication-independent deposition of H3.3 (Drane et al., 2010; Lewis et al., 2010). DAXX harbors an N-terminal DAXX helical bundle (DHB), a histone-binding domain (HBD) in the middle, and a C-terminal intrinsically disordered region (Fig. 1A). The DHB domain reportedly recognizes a consensus motif of different DAXX binding partners (Escobar-Cabrera et al., 2010). The HBD domain harbors histone chaperone activity and specifically envelops the histone H3.3-H4 dimer for H3.3-specific recognition (Elsasser et al., 2012; Liu et al., 2012).

ATRX was discovered to map the genetic mutations that lead to the α-thalassemia, mental retardation, X-linked (ATRX) syndrome (Gibbons et al., 1995). This ATP-dependent chromatin remodeling protein contains an N-terminal ATRX-DNMT3-DNMT3L (ADD) domain, partner-binding regions in the middle and a C-terminal ATPase domain (Fig. 1A). The ADD domain functions as a reader module that recognizes histone H3 “K4me0-K9me3” methylation pattern and tolerates additional H3S10 phosphorylation to facilitate heterochromatin targeting of ATRX (Iwase et al., 2011; Noh et al., 2015). Regions for binding macroH2A, EZH2, HP1, DAXX, and MeCP2 have been identified in ATRX. These interactions contribute to the cellular localization and activities of ATRX (Ratnakumar and Bernstein, 2013).

ATRX physically interacts with DAXX to promote the incorporation of H3.3 into telomeric, pericentromeric, and other repetitive DNA regions (Drane et al., 2010; Goldberg et al., 2010; Lewis et al., 2010). Under conditions of DNA hypomethylation, DAXX-ATRX complex is essential to promote H3K9 trimethylation around the tandem repetitive elements, thus safeguarding the genome stability in embryonic stem cells (He et al., 2015). The interaction regions between DAXX and ATRX have been mapped to the DHB domain of DAXX (DHB_{DAXX}, aa 55–144) and the DAXX interaction domain of ATRX (DID_{ATRX}, aa 1,189–1,326) (Fig. 1A) (Tang et al., 2004).

To further map the minimal region of DID_{ATRX} essential for DAXX interaction, we generated a series of DID_{ATRX} truncations based on secondary structural analysis, and performed isothermal titration calorimetry (ITC) studies (Fig. 1B). We measured a dissociation constant (K_D) of 4.5 μmol/L between full length DID_{ATRX} (aa 1,189–1,326) and DHB_{DAXX}. Strikingly, we detected a binding K_D of 70 nmol/L between a 42-residue segment of DID_{ATRX} and DHB_{DAXX}. This segment is characteristic of a loop-helix motif and spans residues 1,244–1,285 of ATRX (Fig. 1A). The observed ~64-fold enhancement of affinity underscores the binding potency of $ATRX_{1,244–1,285}$, and suggests an autoinhibitory role of the $ATRX_{1,244–1,285}$-flanking sequence. The binding K_D dropped to 1 μmol/L when the α-helix frame only (α_{DID}, $ATRX_{1,265–1,285}$) was used for ITC titration, stressing the role of loop $ATRX_{1,244–1,264}$ in promoting DAXX-ATRX interaction.

We next co-expressed, purified, crystallized the complex of DHB_{DAXX}-$ATRX_{1,244–1,285}$, and solved the crystal structure at 1.58 Å by zinc single wavelength anomalous dispersion (Table S1). Full length DHB_{DAXX} and residues 1,256–1,285 of ATRX were modelled based on the electron density map (Fig. S1). DHB_{DAXX} features a core four-helical bundle and $ATRX_{1,256–1,285}$ adopts a loop-helix fold that targets the “α2-α5” surface of DHB_{DAXX} (Fig. 1C). In the crystal, the modelled DHB_{DAXX}-$ATRX_{1,256–1,285}$ complex forms a “head-to-head” dimer organized around the α3 linker helix of DHB_{DAXX} (Fig. S2A). Despite extensive interactions, our SEC-MALS (size exclusion chromatography followed by multi-angle light scattering) analysis suggested that the DHB_{DAXX}-$ATRX_{1,244–1,285}$ complex exists as a monomer in solution and the observed dimer formation is likely due to crystal packing (Fig. S2B and S2C). The free and complex states of DHB_{DAXX} are well superimposable without clear conformational change (Fig. S2D), suggesting that the ATRX

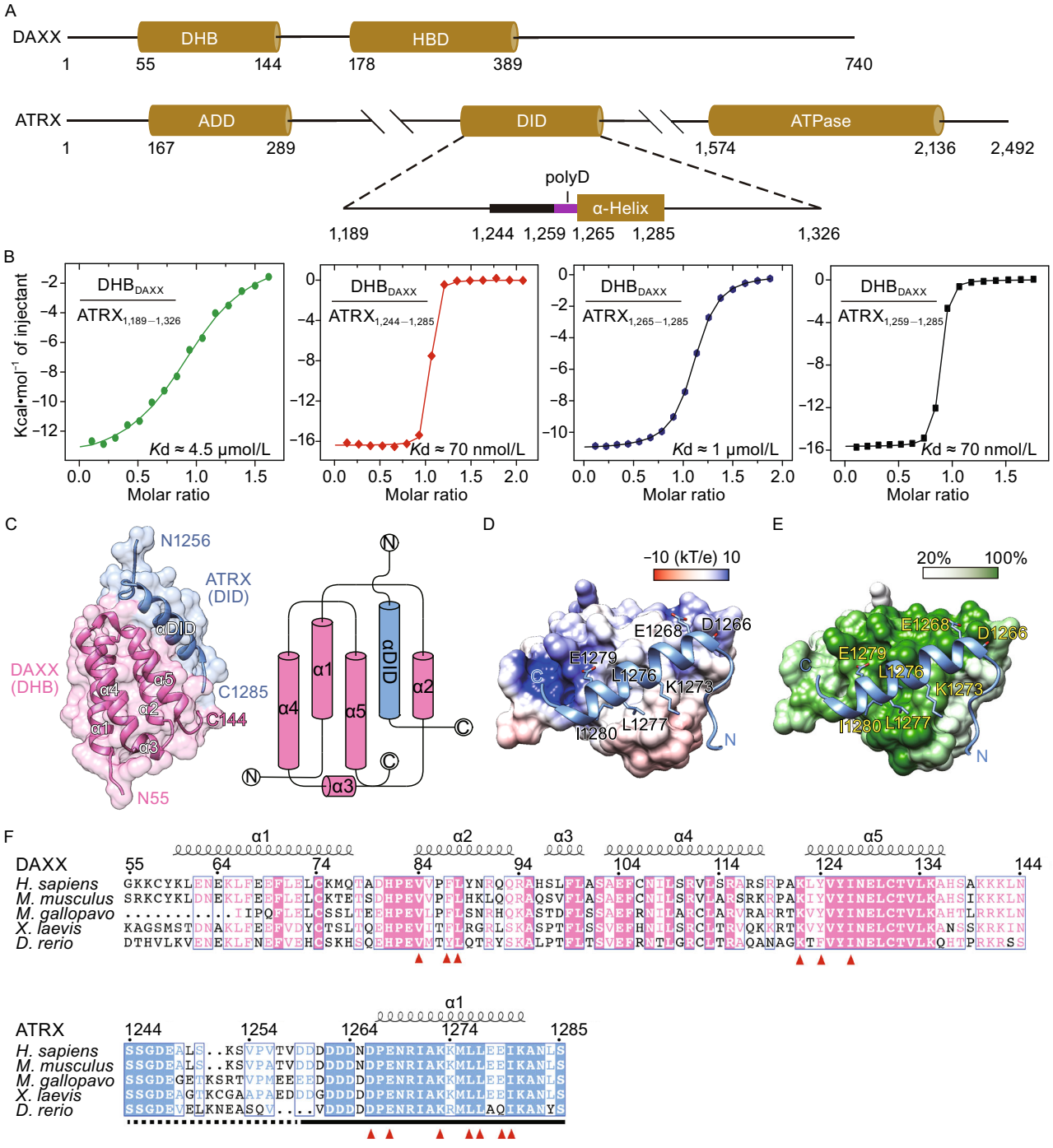

Figure 1. Overall structure of DAXX-ATRX mini-complex. (A) The domain architecture of DAXX and ATRX. (B) ITC fitting curves of the DHB domain of DAXX (DHB_{DAXX}) titrated with $ATRX_{1,189–1,326}$, $ATRX_{1,244–1,285}$, $ATRX_{1,265–1,285}$, and $ATRX_{1,259–1,285}$. (C) Surface and topological representation of DAXX-ATRX mini-complex. DHB_{DAXX} and $ATRX_{1,256–1,285}$ peptide are coded pink and blue, respectively. (D) Electrostatic potential surface view of the DAXX-ATRX mini-complex. DAXX is colored as a spectrum of its surface electrostatic potential ranging from blue (10 kT/e) to red (−10 kT/e). (E) Conservation mapping surface view of the DAXX-ATRX mini-complex. DAXX is colored based on the surface conservation score among orthologs aligned in panel (F). (F) Sequence alignment of DAXX and ATRX orthologs in vertebrates. Red triangles, key residues participating in DAXX-ATRX interaction. Dashed lines, invisible sequence in the crystal structure.

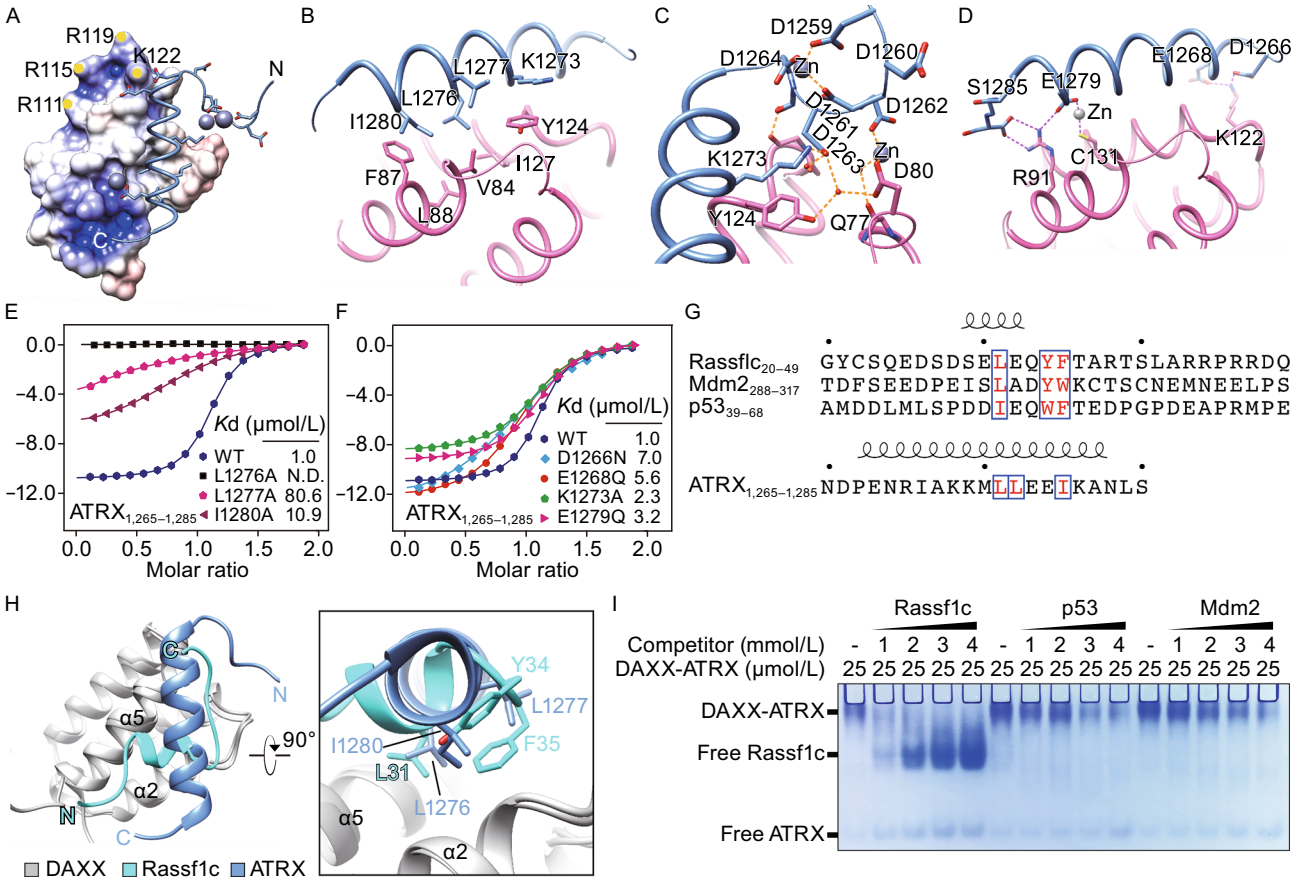

Figure 2. Interaction details, mutagenesis study and competition assay. (A) Positioning of ATRX loop-helix motif on DHB_{DAXX}. DHB_{DAXX} is in electrostatic potential surface view as defined in Fig. 1D. ATRX is in ribbon representation with key residues in stick view. Yellow dots denote the positions of four annotated basic residues. Grey spheres, zinc ions. (B) Details of hydrophobic contacts between DHB_{DAXX} (pink) and ATRX α-helix (blue). Key residues are shown in stick view. (C) Details of hydrophilic contact involving the polyD loop of ATRX (blue). Gray spheres, zinc ions; small red balls, water molecules; dashed lines, hydrogen bonds. (D) Details of hydrophilic interactions involving ATRX α-helix (blue). (E and F) ITC fitting curves of DHB_{DAXX} titrated with denoted $ATRX_{1,265–1,285}$ mutant peptides. WT, wild type peptide control. (G) Sequence alignment among Rassf1c (20–49), Mdm2 (288–317), and p53 (39–68), and ATRX (1,265–1,285) peptides. Blue boxes highlight key hydrophobic residues of the consensus motif. (H) Structural superimposition of DHB_{DAXX}-Rassf1c with DHB_{DAXX}-ATRX. DHB_{DAXX}, Rassf1c, and ATRX peptides are colored gray, cyan and blue, respectively. Right, "close-up" view of the central hydrophobic core. Key hydrophobic residues are depicted as sticks. (I) Electrophoretic mobility shift assay to detect the disassociation of preformed DAXX-ATRX complex upon incubation with denoted competitor peptides. Protein bands are detected by Coomassie blue staining. Only DAXX-ATRX, free Rassf1c, and free ATRX peptides can enter the gel and are labelled accordingly. Frame information are as the follows: DAXX, 55–144; ATRX, 1,244–1,285; Rassf1c, 20–44; p53, 39–63; Mdm2, 293–317.

binding surface of DHB_{DAXX} is largely preformed. Since only $ATRX_{1,259–1,285}$ is visible in the complex structure, we next tested if this short motif is sufficient for DAXX binding. A binding K_D of 70 nmol/L was measured between $ATRX_{1,259–1,285}$ and DHB_{DAXX} (Fig. 1B), which is nearly the same as $ATRX_{1,244–1,285}$. Thus, our structural studies further defined a minimum ATRX motif of only 27 residues for high affinity DAXX interaction. Electrostatic potential analysis revealed that $ATRX_{1,259–1,285}$ covers an elongated surface that is hydrophobic in the center flanked by electrostatic positive patches (Fig. 1D). Upon complex formation, we calculated a buried solvent accessible area of 1,111 $Å^2$, which accounts for ~18% of the total solvent accessible area of DHB_{DAXX}. Residues constituting the ATRX binding surface of DAXX are highly conserved among vertebrate species ranging from zebrafish to human (Fig. 1E and 1F), highlighting their functional consensus.

$ATRX_{1,259–1,285}$ engages extensive interactions with DHB_{DAXX} to form a compact five-helical bundle (Figs. 1C and 2A). These interactions can be classified into three groups including a central hydrophobic core and two flanking polar clusters. The central hydrophobic core is composed of

V84, F87, L88, Y124 and I127 of DAXX and L1276, L1277, I1280, K1273 (via its hydrocarbon portion) of ATRX (Fig. 2B). Human $ATRX_{1,259–1,285}$ is characteristic of an N-terminal polyD loop ($_{1,259}DDDDDD_{1,264}$) (Fig. 1F). Deletion of the polyD loop led to an affinity drop from 70 nmol/L to 1 μmol/L (Fig. 1B), stressing its binding contribution. Notably, the polyD loop is structurally organized by zinc coordination (involving residues D1259, D1261, D1264, D1262) and intra-ion pair formation (D1263-K1273) (Fig. 2C). This stabilized structural unit of polyD loop further interacts with DHB_{DAXX} via a network of water-mediated hydrogen-bonding interactions (Fig. 2C). Next to the polyD loop is a positive surface patch formed by residues R111, R115, R119 and K122 of DAXX (Fig. 2A), which may electrostatically facilitate DAXX-ATRX interaction. Particularly, K122 directly pairs with E1268 and D1266 of ATRX to facilitate binding (Fig. 2D). The other set of polar cluster is formed around the C-terminal part of the loop-helix motif of ATRX. In particular, these interactions include a unique zinc finger coordination involving residues E1279 of ATRX and C131 of DAXX, as well as ion pairs between R91 of DAAX and S1285, E1279 of ATRX (Fig. 2D).

Next, we synthesized mutant ATRX peptides in the frame of 1,265–1,285, and performed ITC study to validate the observed interactions. As expected, L1276A completely disrupt DBH_{DAXX} binding, while the binding K_D dropped from 1 μmol/L to 80.6 μmol/L for L1277A and 10.9 μmol/L for I1280A (Fig. 2E). Consistent with our structural analysis, the K_D values dropped 2.3- to 7-fold between DBH_{DAXX} and different ATRX polar residue mutants such as D1266N, E1268Q, K1273A and E1279Q (Fig. 2F). The more pronounced binding loss in the cases of L1276A, L1277A and I1280A underscores a critical role of the hydrophobic core to nucleate DAXX-ATRX interaction.

Besides ATRX, DHB_{DAXX} also interacts with other partners, such as Rassf1c, Mdm2, and p53 that share a consensus motif (Fig. 2G). The NMR solution structure of DHB_{DAXX}-Rassf1c complex has been reported (Escobar-Cabrera et al., 2010). Structural alignment revealed that ATRX and Rassf1c target the same “α2-α5” surface of DHB_{DAXX} (Fig. 2H). Interestingly, the ATRX and Rassf1c peptides adopt distinct conformations for DHB_{DAXX} targeting. As shown in Fig. 2H, the helix elements of ATRX and Rassf1c are almost perpendicular to each other. The most conserved binding feature is the central hydrophobic core that is contributed by residues L1276, L1277, I1280 in the case of ATRX and residues L31, Y34, F35 in the case of Rassf1c (Fig. 2H). Notably, a leucine residue is structurally conserved in both ATRX (L1276) and Rassf1c (L31), and is anchored at the central hydrophobic pocket of DHB_{DAXX} to nucleate binding.

DAXX and ATRX form a complex in promyelocytic leukemia (PML) nuclear bodies and heterochromatin to regulate gene activity and chromatin structure. DAXX recruits Rassf1C into PML nuclear bodies and releases it when DAXX is degraded upon DNA damage (Kitagawa et al., 2006). DAXX interacts with the E3 ligase Mdm2 in PML nuclear bodies and prevents its self-ubiquitination, thus mediating the proteolytic degradation of p53 (Tang et al., 2006). DAXX also interacts with p53 to regulate its activity by competitive interaction with PML (Kim et al., 2003). Given the shared binding mode and cellular localization of the abovementioned DAXX partners, it is interesting to explore their competitive feature. To this end, we performed peptide competition assays based on electrophoretic mobility shift assay. The preformed DHB_{DAXX}-$ATRX_{1,244–1,285}$ complex was incubated with competitor peptides ($Rassf1c_{20–44}$, $p53_{39–63}$ and $Mdm2_{293–317}$) of different concentration, and then subjected to native-PAGE analysis. As shown in Fig. 2I, the DAXX-ATRX complex was gradually disrupted by the competitor peptides in a concentration-dependent manner, among which the Rassf1c peptide displayed the strongest competitor activity, followed by p53 and Mdm2 peptides. These results indicate that ATRX, Rassf1c, Mdm2, and p53 bind to DAXX in a mutually exclusive manner and they likely compete for DAXX interaction under regulated conditions, thus suggesting a “partner switch” mechanism in DAXX biology.

FOOTNOTES

The atomic coordinate and structure factor of $DAXX_{55–144}$-$ATRX_{1,244–1,285}$ complex have been deposited in the Protein Data Bank with accession numbers of 5GRQ.

We thank Dr. Jiahuai Han at Xiamen University for providing the cDNA of DAXX. We thank the staff members at beamline BL19U1 of the Shanghai Synchrotron Radiation Facility and Dr. S. Fan at Tsinghua Center for Structural Biology for their assistance in data collection and the China National Center for Protein Sciences Beijing for providing facility support. This work was supported by grants from the Ministry of Science and Technology of China (2016YFA0500700 and 2015CB910503), the National Natural Science Foundation of China (Grant No. 31270763), the Tsinghua University Initiative Scientific Research Program to H.L, and the National Postdoctoral Program for Innovative Talents (BX201600088) to D.Z. D.Z. is a postdoctoral fellow of Tsinghua-Peking Joint Center for Life Sciences.

H.L. conceived and designed the study. Z.L. designed and conducted the experiments with help from D.Z. and B.X. H.L. and Z.L. analyzed the data and wrote the paper.

Zhuang Li, Dan Zhao, Bin Xiang, and Haitao Li declare that they have no conflict of interest.

This article does not contain any studies with human or animal subjects performed by any of the authors.

Zhuang Li[1,2], Dan Zhao[2], Bin Xiang[1,2], Haitao Li[2]✉

[1] College of Life Sciences, Peking University, Beijing 100871, China
[2] MOE Key Laboratory of Protein Sciences, Tsinghua-Peking Joint Center for Life Sciences, Beijing Advanced Innovation Center for Structural Biology, Department of Basic Medical Sciences, School of Medicine, Tsinghua University, Beijing 100084, China
✉ Correspondence: lht@tsinghua.edu.cn (H. Li)

REFERENCES

Drane P, Ouararhni K, Depaux A, Shuaib M, Hamiche A (2010) The death-associated protein DAXX is a novel histone chaperone involved in the replication-independent deposition of H3.3. Genes Dev 24:1253–1265

Elsasser SJ, Huang H, Lewis PW, Chin JW, Allis CD, Patel DJ (2012) DAXX envelops a histone H3.3-H4 dimer for H3.3-specific recognition. Nature 491:560–565

Escobar-Cabrera E, Lau DK, Giovinazzi S, Ishov AM, McIntosh LP (2010) Structural characterization of the DAXX N-terminal helical bundle domain and its complex with Rassf1C. Structure 18:1642–1653

Gibbons RJ, Picketts DJ, Villard L, Higgs DR (1995) Mutations in a putative global transcriptional regulator cause X-linked mental retardation with alpha-thalassemia (ATR-X syndrome). Cell 80:837–845

Goldberg AD, Banaszynski LA, Noh KM, Lewis PW, Elsaesser SJ, Stadler S, Dewell S, Law M, Guo X, Li X et al (2010) Distinct factors control histone variant H3.3 localization at specific genomic regions. Cell 140:678–691

He Q, Kim H, Huang R, Lu W, Tang M, Shi F, Yang D, Zhang X, Huang J, Liu D et al (2015) The Daxx/Atrx complex protects tandem repetitive elements during DNA hypomethylation by promoting H3K9 trimethylation. Cell Stem Cell 17:273–286

Iwase S, Xiang B, Ghosh S, Ren T, Lewis PW, Cochrane JC, Allis CD, Picketts DJ, Patel DJ, Li H et al (2011) ATRX ADD domain links an atypical histone methylation recognition mechanism to human mental-retardation syndrome. Nat Struct Mol Biol 18:769–776

Kim EJ, Park JS, Um SJ (2003) Identification of Daxx interacting with p73, one of the p53 family, and its regulation of p53 activity by competitive interaction with PML. Nucleic Acids Res 31:5356–5367

Kitagawa D, Kajiho H, Negishi T, Ura S, Watanabe T, Wada T, Ichijo H, Katada T, Nishina H (2006) Release of RASSF1C from the nucleus by Daxx degradation links DNA damage and SAPK/JNK activation. EMBO J 25:3286–3297

Lewis PW, Elsaesser SJ, Noh KM, Stadler SC, Allis CD (2010) Daxx is an H3.3-specific histone chaperone and cooperates with ATRX in replication-independent chromatin assembly at telomeres. Proc Natl Acad Sci USA 107:14075–14080

Liu CP, Xiong C, Wang M, Yu Z, Yang N, Chen P, Zhang Z, Li G, Xu RM (2012) Structure of the variant histone H3.3-H4 heterodimer in complex with its chaperone DAXX. Nat Struct Mol Biol 19:1287–1292

Noh KM, Maze I, Zhao D, Xiang B, Wenderski W, Lewis PW, Shen L, Li H, Allis CD (2015) ATRX tolerates activity-dependent histone H3 methyl/phos switching to maintain repetitive element silencing in neurons. Proc Natl Acad Sci USA 112:6820–6827

Ratnakumar K, Bernstein E (2013) ATRX: the case of a peculiar chromatin remodeler. Epigenetics 8:3–9

Tang J, Wu S, Liu H, Stratt R, Barak OG, Shiekhattar R, Picketts DJ, Yang X (2004) A novel transcription regulatory complex containing death domain-associated protein and the ATR-X syndrome protein. J Biol Chem 279:20369–20377

Tang J, Qu LK, Zhang J, Wang W, Michaelson JS, Degenhardt YY, El-Deiry WS, Yang X (2006) Critical role for Daxx in regulating Mdm2. Nat Cell Biol 8:855–862

Electronic supplementary material The online version of this article (doi:10.1007/s13238-017-0463-x) contains supplementary material, which is available to authorized users.